Mineralogical Magazine (2019), **83**, 607–614
doi:10.1180/mgm.2018.171

CAMBRIDGE UNIVERSITY PRESS

Article

Stefanweissite, $(Ca,REE)_2Zr_2(Nb,Ti)(Ti,Nb)_2Fe^{2+}O_{14}$, a new zirconolite-related mineral from the Eifel paleovolcanic region, Germany

Nikita V. Chukanov[1]*, Natalia V. Zubkova[2], Igor V. Pekov[2,3], Marina F. Vigasina[2], Yury S. Polekhovsky[4], Bernd Ternes[5], Willi Schüller[6], Sergey N. Britvin[4,7] and Dmitry Yu. Pushcharovsky[2]

[1]Institute of Problems of Chemical Physics, Russian Academy of Sciences, Chernogolovka, Moscow region, 142432 Russia; [2]Faculty of Geology, Moscow State University, Vorobievy Gory, 119991 Moscow, Russia; [3]Vernadsky Institute of Geochemistry and Analytical Chemistry, Russian Academy of Sciences, Kosygin str. 19, 119991 Moscow, Russia; [4]Institute of Earth Sciences, St Petersburg State University, Universitetskaya Nab. 7/9, 199034 St Petersburg, Russia; [5]Bahnhofstrasse 45, 56727 Mayen, Germany; [6]Im Straußenpesch 22, 53518 Adenau, Germany; and [7]Nanomaterials Research Center, Kola Science Centre, Russian Academy of Sciences, Fersman str. 14, 184209 Apatity, Murmansk region, Russia

Abstract

The new mineral stefanweissite, IMA2018-020, was discovered in sanidinite volcanic ejecta from the Laach Lake (Laacher See) paleovolcano, Eifel region, Rhineland-Palatinate, Germany. Associated minerals are sanidine, nosean, biotite, augite, titanite, ferriallanite-(La), magnetite, baddeleyite and a pyrochlore-group mineral. Stefanweissite is brown and reddish-brown, with adamantine lustre; the streak is light brown to yellow. It forms long-prismatic crystals up to 0.03 mm × 0.07 mm × 1.0 mm and acicular crystals up to 2 mm long and 0.02 mm thick typically combined in radiated aggregates in cavities in sanidinite. $D_{calc.}$ = 5.254 g/cm^3. The mean refractive index calculated from the Gladstone–Dale equation is 2.260. The Raman spectrum shows the absence of hydrogen-bearing groups. The chemical composition is (electron microprobe, wt.%): CaO 7.63, MnO 2.51, FeO 7.86, Al_2O_3 0.25, La_2O_3 2.28, Ce_2O_3 6.54, Pr_2O_3 1.01, Nd_2O_3 1.59, ThO_2 3.71, UO_2 1.09, TiO_2 17.32, ZrO_2 28.03, HfO_2 0.91, Nb_2O_5 19.96, total 99.69. The empirical formula based on 14 O atoms per formula unit is $Ca_{1.13}(Ce_{0.33}La_{0.12}Nd_{0.08}Pr_{0.05})_{\Sigma 0.58}Th_{0.12}U_{0.03}Mn_{0.29}Fe_{0.91}Al_{0.04}Zr_{1.89}Hf_{0.04}Ti_{1.80}Nb_{1.19}O_{14}$. The simplified formula is $(Ca,REE)_2Zr_2(Nb,Ti)(Ti,Nb)_2Fe^{2+}O_{14}$. Stefanweissite is orthorhombic, with space group *Cmca*. The unit-cell parameters are: a = 7.2896(4) Å, b = 14.1435(5) Å, c = 10.1713(4) Å and V = 1048.68(7) Å^3. The crystal structure was solved using single-crystal X-ray diffraction data. Stefanweissite is an analogue of zirconolite-3*O* with Nb dominant over Ti in one of two octahedral sites. The strongest lines of the powder X-ray diffraction pattern [*d*, Å (*I*, %) (*hkl*)] are: 2.983(100)(202), 2.897(71)(042), 1.828(38)(154, 400, 333), 1.793(25)(244), 1.767(16)(080), 1.517(10)(282), 1.187(19)(483, 1.11.3, 602). Type material is deposited in the collections of the Fersman Mineralogical Museum of the Russian Academy of Sciences, Moscow, Russia, with the registration number 5191/1.

Keywords: stefanweissite, new mineral, zirconolite, laachite, nöggerathite-(Ce), sanidinite, crystal structure, alkaline volcanic rock, Laacher See, Eifel

(Received 4 September 2018; accepted 14 December 2018; Accepted Manuscript online: 21 January 2019; Associate Editor: Anthony R Kampf)

Introduction

Thorium, uranium and rare-earth-element (*REE*) minerals are of interest as possible prototypes of nuclear waste forms (Lumpkin *et al.*, 2014). In particular, synthetic materials chemically and structurally related to zirconolite are considered as potential components of advanced materials which can be used for durable containment of high-level radioactive wastes, including trivalent and tetravalent actinides, such as unrecyclable plutonium, as well as neptunium, curium and americium (Ringwood *et al.*, 1986; Donald *et al.*, 1997; Laverov *et al.*, 2006; Barinova *et al.*, 2008; Zhang *et al.*, 2017). As a rule, in nature zirconolite-group minerals contain uranium and thorium, the total content of which can reach 15–20 wt.% (Williams and Gieré, 1996; Hurai *et al.*, 2018).

Zirconolite-type minerals exhibit significant structural and chemical diversity. Currently, there are four minerals (one with three polytypes) belonging to this family: zirconolite-3*O* (formerly polymignite) $(Ca,REE)_2Zr_2(Ti,Nb)_3FeO_{14}$, zirconolite-3*T* $(Ca,REE)_2Zr_2(Ti,Nb)_3FeO_{14}$, zirconolite-2*M* $(Ca,REE)_2Zr_2(Ti,Nb)_3FeO_{14}$, laachite $Ca_2Zr_2Nb_2TiFeO_{14}$, nöggerathite-(Ce) $(Ce,Ca)_2Zr_2(Nb,Ti)(Ti,Nb)_2Fe^{2+}O_{14}$, and described in this paper stefanweissite $(Ca,REE)_2Zr_2(Nb,Ti)(Ti,Nb)_2Fe^{2+}O_{14}$. Zirconolite-3*O* $(Ca,REE)_2Zr_2(Ti,Nb)_3FeO_{14}$ and zirconolite-3*T* are the most common zirconolite-type species. Laachite, nöggerathite-(Ce) and stefanweissite discovered in sanidinites of the Laach Lake area are rare. Unlike most other samples of zirconolite-type minerals, they

*Author for correspondence: Nikita V. Chukanov, Email: chukanov@icp.ac.ru
Cite this article: Chukanov N.V., Zubkova N.V., Pekov I.V., Vigasina M.F., Polekhovsky Y.S., Ternes B., Schüller W., Britvin S.N. and Pushcharovsky D.Y.u. (2019) Stefanweissite, $(Ca,REE)_2Zr_2(Nb,Ti)(Ti,Nb)_2Fe^{2+}O_{14}$, a new zirconolite-related mineral from the Eifel paleovolcanic region, Germany. *Mineralogical Magazine* **83**, 607–614. https://doi.org/10.1180/mgm.2018.171

Fig. 1. Aggregates of brown lath- and needle-shaped crystals of stefanweissite on sanidine, in association with biotite (*a*, *c*) and magnetite (*b*). Photographer: Stefan Wolfsried. Field of view widths: (*a*) 1 mm; (*b*) 1.5 mm; (*c*) 0.8 mm; and (*d*) 2 mm.

are non-metamict being crystallised not earlier than a few dozens of million years ago. (Litt *et al.*, 2001; Schmitt *et al.*, 2010).

The new mineral species stefanweissite is named in honour of PhD Stefan Weiss (b. 1955), German geologist, mineralogist and petrologist, and editor of the *LAPIS* magazine since May 1993, effectively promoting mineralogy among collectors and amateurs. From 1979 to 2017, Stefan Weiss has published more than 180 articles in *LAPIS* on general and descriptive mineralogy, classic mineral localities, regional mineralogy and new finds in the Alps, Cornwall and Saxony. He regularly edits the *LAPIS* magazine series 'Neue Mineralien' which has presented, since 1992, more than 1550 abstracts on new mineral species. Stefan Weiss is also an author of several books including those about German mineral localities.

The new mineral stefanweissite and its name were approved by the International Mineralogical Association (IMA) Commission on New Minerals, Nomenclature and Classification (CNMNC) (|IMA2018-020, Chukanov *et al.*, 2018*c*). The type specimen is deposited in the collection of the Fersman Mineralogical Museum of the Russian Academy of Sciences, Moscow, Russia, with the registration number 5191/1.

Occurrence, general appearance and mechanical properties

Stefanweissite occurs in the In den Dellen (Zieglowski) pumice quarry (50°23′40″N, 7°17′12″E), 1.5 km NE of Mendig, Laach Lake (Laacher See) volcano, Eifel region, Rhineland-Palatinate, Germany. It forms isolated flattened long-prismatic crystals up to 0.03 mm × 0.07 mm × 1.0 mm and acicular crystals up to 2 mm long and 0.02 mm thick typically combined in radiated aggregates (Fig 1) in cavities inside sanidinite volcanic ejecta. Usually, the dominant crystal form is {001} and other forms are {011}, {010}, {111), as well as occasionally {100}. Associated minerals are sanidine, nosean, biotite, augite, titanite, ferriallanite-(La), magnetite, baddeleyite and a pyrochlore-group mineral.

Crystals of stefanweissite are translucent to transparent. The colour is brown, reddish-brown to very dark brownish-red, with red–brown internal reflections; some thin needles are yellowish-brown. The lustre is adamantine. The streak is light brown to yellow. No cleavage is observed; the fracture is uneven. Density could not be measured due to the absence of heavy liquids with $D > 5$ g cm^{-3} and insufficient amount of material to measure density by hydrostatic weighing or volumetric methods. Density calculated using the empirical formula is 5.254 g cm^{-3}.

https://doi.org/10.1180/mgm.2018.171 Published online by Cambridge University Press

Table 1. Reflectance values (R_{max}/R_{min}) for stefanweissite.

λ (nm)	R_{max}	R_{min}	λ (nm)	R_{max}	R_{min}
400	16.6	15.5	560	15.4	14.1
420	16.4	15.2	580	15.2	14.0
440	16.2	15.0	**589**	**15.2**	**13.89**
460	16.1	14.8	600	15.1	13.8
470	**16.0**	**14.7**	620	15.0	13.7
480	15.9	14.6	640	14.78	13.6
500	15.8	14.4	**650**	**14.7**	**13.5**
520	15.6	14.3	660	14.6	13.4
540	15.5	14.2	680	14.5	13.3
546	**15.5**	**14.2**	700	14.4	13.2

Reflectance values for four wavelengths recommended by the IMA Commission on Ore Microscopy are given in bold type.

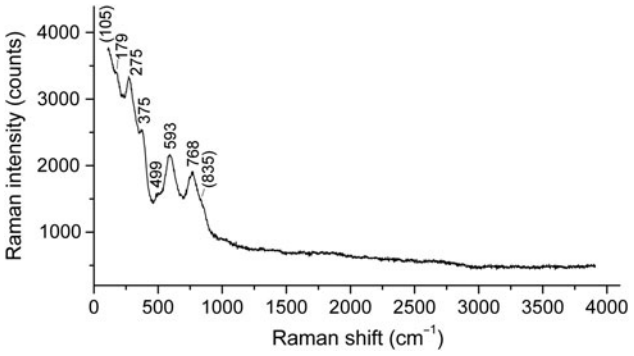

Fig. 2. Raman spectrum of stefanweissite.

Optical properties

Reflectance values for stefanweissite have been measured in air using a MSF-21 micro-spectrophotometer (LOMO company, St. Petersburg, Russia) with the monochromator slit width of 0.4 mm and beam diameter of 0.1 mm. SiC (Reflection standard 474251, No. 545, Germany) was used as a standard. The reflectance values (R_{max}/R_{min}) are given in Table 1.

In reflected light, stefanweissite is anisotropic, with ΔR_{589} = 1.27%. The mineral is light grey, with brown internal reflections.

The mean *n* value, calculated from the Gladstone–Dale equation using the empirical formula and the calculated density, is 2.260.

Raman spectroscopy

The Raman spectrum of a randomly oriented stefanweissite crystal (Fig. 2) was obtained using an EnSpectr R532 spectrometer based on an OLYMPUS CX 41 microscope coupled with a diode laser (λ = 532 nm) at room temperature. The spectrum was recorded in the range from 100 to 4000 cm^{-1} with a diffraction grating (1800 gr mm^{-1}) and spectral resolution ~6 cm^{-1}. The output power of the laser beam was ~9 mW. The diameter of the focal spot on the sample was <10 μm. The back-scattered Raman signal was collected with 40× objective; signal acquisition time for a single scan of the spectral range was 2 s and the signal was averaged over 100 scans.

The Raman spectrum of stefanweissite shows the absence of bands of H_2O molecules (in the ranges 2500–3800 and 1500–700 cm^{-1}), OH groups (2500–3800 cm^{-1}) and CO_3^{2-} anions (1040–1100 cm^{-1}). According to Salamat *et al.* (2013), the band at 768 cm^{-1} with the shoulder at 835 cm^{-1} is to be assigned to symmetric stretching vibrations of TiO_6 groups in the zirconolite-type structure. By analogy with monoclinic ZrO_2 (Geisler *et al.*, 2003), the band at 593 cm^{-1} can be assigned to Zr–O-stretching vibrations. The bands below 400 cm^{-1} correspond to lattice modes involving (Ca,*REE*)–O-stretching and O–(Ti,Nb,Zr)–O bending vibrations.

Table 2. Chemical composition of stefanweissite.

Constituent	Wt.%	Range	S.D.	Standard
CaO	7.63	6.53–8.52	0.69	Wollastonite
MnO	2.51	2.07–2.80	0.29	$MnTiO_3$
FeO	7.86	6.97–8.68	0.57	Fe
Al_2O_3	0.25	0–0.53	0.22	Albite
La_2O_3	2.28	1.85–2.74	0.31	$LaPO_4$
Ce_2O_3	6.54	5.46–7.49	0.74	$CePO_4$
Pr_2O_3	1.01	0.80–1.28	0.17	$PrPO_4$
Nd_2O_3	1.59	1.27–1.80	0.20	$NdPO_4$
ThO_2	3.71	3.24–4.16	0.28	ThO_2
UO_2	1.09	0.82–1.31	0.19	UO_2
TiO_2	17.32	16.73–19.10	0.86	TiO_2
ZrO_2	28.03	26.55–29.16	0.94	ZrO_2
HfO_2	0.91	0.72–1.11	0.12	$HfSiO_4$
Nb_2O_5	18.96	17.86–19.88	0.69	$LiNbO_3$
Total	99.69			

S.D. – Standard deviation

Chemical data

The chemical composition of the new mineral was determined using an Oxford INCA Wave 700 electron microprobe (wavelength-dispersive spectroscopy mode, 20 kV, 600 pA and 300 nm beam diameter). Analytical data (average of seven spot analyses) are given in Table 2. Contents of other elements with atomic numbers >8 are below detection limits. On the basis of structural data (see below) and by analogy with the related mineral laachite (Chukanov *et al.*, 2014), iron and manganese are considered as Fe^{2+} and Mn^{2+}, respectively.

The empirical formula based on 14 O atoms per formula unit (apfu) (in accordance with structural data, $Z = 4$) is $Ca_{1.13}(Ce_{0.33}La_{0.12}Nd_{0.08}Pr_{0.05})_{\Sigma 0.58}Th_{0.12}U_{0.03}Mn_{0.29}Fe_{0.91}Al_{0.04}Zr_{1.89}Hf_{0.04}Ti_{1.80}Nb_{1.19}O_{14}$. The simplified formula is (Ca, *REE*)$_2$Zr$_2$(Nb,Ti)(Ti,Nb)$_2$$Fe^{2+}O_{14}$.

X-ray diffraction and crystal structure

Powder X-ray diffraction data were collected using a Rigaku RAXIS Rapid II diffractometer with a curved image plate detector, rotating anode, and in Debye–Scherrer geometry. The accelerating voltage = 40 kV, current = 15 mA and exposure = 15 min. The distance between sample and detector was 127.4 mm. Data (in Å for Co*K*α) are listed in Table 3.

Diffraction peaks are indexed agreeably in the orthorhombic unit cell, space group *Cmca*. The unit-cell parameters calculated from the powder data are: $a = 7.285(2)$ Å, $b = 14.141(3)$ Å, $c = 10.166(2)$ Å and $V = 1047(1)$ Å^3.

Single-crystal X-ray studies were carried out using an XCaliburS CCD diffractometer, using Mo*K*α radiation (λ = 0.71073 Å). For crystal data, data collection information and structure refinement details see Table 4. Site coordinates, equivalent thermal displacement parameters, site populations and site multiplicities are given in Table 5; selected interatomic distances are listed in

https://doi.org/10.1180/mgm.2018.171 Published online by Cambridge University Press

Table 3. Powder X-ray diffraction data for stefanweissite.

I_{obs}	I_{calc}*	d_{obs}	d_{calc}**	*h k l*
4	2	4.121	4.129	0 2 2
8	12	3.682	3.689	1 3 1
4	2	3.335	3.340	0 4 1
100	**100**	**2.983**	**2.963**	**2 0 2**
71	**93**	**2.897**	**2.903**	**0 4 2**
3	1	2.571	2.575	1 3 3
3	1	2.370	2.367	1 1 4
2	5	2.338	2.342	2 2 3
4	3	2.293	2.296	0 6 1
2	1	2.135	2.139	1 3 4
2	2	2.111	2.113	3 3 1
2	1	2.080	2.082	1 5 3
3	1	1.993	2.000	2 2 4
1	1	1.935	1.935	0 6 3
4	5	1.911	1.912	1 7 1
38	**1, 17, 2**	**1.828**	**1.830, 1.822, 1.822**	**1 5 4, 4 0 0, 3 3 3**
25	**61**	**1.793**	**1.796**	**2 4 4**
16	**12**	**1.767**	**1.768**	**0 8 0**
1	1	1.741	1.742	0 8 1
3	4	1.686	1.688	1 7 3
3	1	1.648	1.646	3 3 4
3	2	1.639	1.640	1 1 6
2	1	1.598	1.600	4 4 1
9	**24, 12, 4**	**1.536**	**1.543, 1.537, 1.536**	**4 4 2, 2 0 6, 3 7 1**
10	**20**	**1.517**	**1.518**	**2 8 2**
4	7	1.451	1.452	0 8 4
19	**1, 3, 7**	**1.187**	**1.188, 1.186, 1.182**	**4 8 3, 1 11 3, 6 0 2**
7	10	1.159	1.160	2 8 6
2	1, 5, 4	1.148	1.149, 1.149, 1.148	5 3 5, 6 4 0, 0 12 2
7	10, 8	1.136	1.137, 1.135	2 4 8, 4 8 4
2	1, 1, 3	1.122	1.123, 1.122, 1.121	0 8 7, 4 2 7, 2 12 0

*For the calculated pattern, only reflections with intensities ≥1 are given; **For the unit-cell parameters calculated from single-crystal data.
The strongest lines are given in bold.

Table 6. The crystallographic information file has been deposited with the Principal Editor of *Mineralogical Magazine* and is available as Supplementary material (see below).

Like other minerals related to zirconolite-3*O*, the crystal structure of stefanweissite demonstrates alternation of two types of bent polyhedral layers, namely an octahedral layer (Fig. 3*a*), and a layer of cations having seven- and eight-fold coordinations: edge-sharing Ca-dominant distorted cubes [the *M*1 site] and Zr-dominant mono-capped octahedra [the *M*2 site] (Fig. 3*b*). The octahedral layer is built by vertex-sharing $M3O_6$ and $M4O_6$ octahedra forming three- and six-membered rings (hexagonal-tungsten-bronze type arrays). The adjacent *M*5 and *M*6 sites have the coordination numbers 4 and 5, respectively. These sites are located in the centres of six-membered rings and are statistically occupied with Fe^{2+} as the major cation (Fig. 3*c*). The *M*1-centred polyhedron shares edges with neighbouring *M*1-centred cubes to form rows along the *a* axis. Similar rows are formed by seven-fold *M*2-centred polyhedra (mono-capped octahedra). Adjacent rows of eight- and seven-fold polyhedra are linked with each other *via* common edges forming a dense layer. A general view of the crystal structure of stefanweissite is shown in Fig. 4.

The refined crystal-chemical formula of stefanweissite is ($Z = 4$, *REE* are modelled by Ce, coordination numbers of cations are indicated with Roman numerals): $^{VIII}(Ca_{0.544}REE_{0.316}Th_{0.08}Mn_{0.06})_2{}^{VII}(Zr_{0.96}Hf_{0.02}Mn_{0.02})_2{}^{VI}(Nb_{0.729(9)}Ti_{0.271(9)})^{VI}(Ti_{0.78}Nb_{0.21}Al_{0.01})_2{}^{IV}(Fe_{0.22}Mn_{0.03})_2{}^{V}(Fe_{0.21}Mn_{0.04})_2O_{14}$.

Discussion

Stefanweissite is isostructural with zirconolite-3*O* and nöggerathite-(Ce) (IMA2017-107 Chukanov *et al.*, 2018*b*) (see Tables 6 and 7). Zirconolite-3*O* was originally described as 'polymignite' (Berzelius, 1824; Brøgger, 1890) and later redefined and renamed (Bayliss *et al.*, 1989; Mazzi and Munno, 1983; Chukhrov and Bonshtedt-Kupletskaya, 1967; Pudovkina *et al.*, 1969). 'Polymignite' is usually metamict and its powder X-ray diffraction pattern can be obtained only after heating. However, all zirconolite-related minerals from sanidinites of the Laach Lake volcano, including laachite, zirconolite-3*T* (Zubkova *et al.*, 2018), nöggerathite-(Ce), and stefanweissite are non-metamict because of their young geological age: the last eruption of the Laach Lake volcano was ~13,000 years ago.

The filling of the *M*5/*M*6 split-site in stefanweissite and noggerathite-(Ce) is similar, but different from that in zirconolite-3*O* and laachite. The resulting U_{eq} value for *M*6 in stefanweissite is significantly higher than that for *M*5 (Table 5) which could be considered as an indication of overestimation of the reported site scattering. On the other hand, the occupation of the *M*6 site in stefanweissite is in accordance with the chemical data and is similar to that in isostructural nöggerathite-(Ce). The high value of U_{eq} in our case may be a result of the further disorder of the *M*6 site along the *a* axis: the analysis of anisotropic values shows a higher value of U^{11} in comparison with U^{22} and U^{33} (Table 5). However we prefer to give the averaged site position because the problem of localisation of the corresponding sub-sites does not have a unique solution.

Other crystalline minerals related to zirconolite-3*O* and occurring in sanidinite of the Laach Lake volcano are nöggerathite-(Ce) (Ce, Ca)$_2$Zr$_2$(Nb,Ti)(Ti,Nb)$_2$$Fe^{2+}O_{14}$ and laachite $Ca_2Zr_2Nb_2TiFeO_{14}$. Laachite is a monoclinic (pseudo-orthorhombic) analogue of zirconolite-3*O* with Nb prevailing over Ti in two octahedral sites (Chukanov *et al.*, 2014).

Nöggerathite-(Ce) (Chukanov *et al.*, 2018*a*) is isostructural with stefanweissite and differs from the latter by the predominance of *REE* over Ca in sites having 8-fold coordination. However the status of these minerals requires a separate discussion.

There are three different rules that are now used in the nomenclature of minerals, including the Levinson rule of combining *REE*, the rule of a dominant component at a site – the dominant-valency rule, and the rule of the main charge-balancing component. Sometimes these rules contradict each other, and we have to decide, what rule has a priority in a given case.

Chemical compositions of 23 samples of zirconolite-type minerals from the Laach Lake volcano have been determined by us. Most of them correspond to stefanweissite with Ca > Σ*REE*.

In the first description of nöggerathite-(Ce) (Chukanov *et al.*, 2018*a*) data on two samples are given. One of them (Sample 1) for which chemical data were obtained and crystal structure was solved, has the crystal-chemical formula $^{VIII}(REE_{0.88}Ca_{0.80}Mn_{0.24}Th_{0.08})^{VII}(Zr_{1.88}Mn_{0.12})^{VI}(Nb_{1.22}Ti_{0.78})^{VI}(Ti_{1.48}Nb_{0.48}Al_{0.04})^{IV}(Fe_{0.48}Mn_{0.08})^{V}(Fe_{0.40}Mn_{0.04})_2O_{14}$ and the following refined unit-cell parameters: $a = 7.2985(3)$, $b = 14.1454(4)$, $c = 10.1607(4)$ Å and $V = 1048.99(7)$ Å^3. Another one (Sample 2) was characterised by chemical, optical and powder X-ray diffraction data, as well as Raman spectroscopy. Its crystal-chemical formula is $(Ce_{0.57}La_{0.19}Nd_{0.12}Pr_{0.05}Y_{0.06})_{\Sigma 0.99}Ca_{0.79}Th_{0.06}Mn_{0.49}Fe_{0.77}Al_{0.10}Zr_{1.89}Ti_{1.96}Nb_{1.00}O_{14}$ and the refined unit-cell parameters are: $a = 7.296(1)$, $b = 14.147(2)$, $c = 10.161(1)$ Å and $V = 1048.9(2)$ Å^3.

https://doi.org/10.1180/mgm.2018.171 Published online by Cambridge University Press

Table 4. Crystal data, data collection information and structure refinement details.

Crystal data	
Formula	$Ca_{1.09}Ce_{0.63}Th_{0.16}Mn_{0.30}Fe_{0.86}Ti_{1.83}Nb_{1.15}Al_{0.02}Zr_{1.92}Hf_{0.04}O_{14}$
Formula weight	835.06
Temperature (K)	293(2)
Crystal system, space group, *Z*	Orthorhombic, *Cmca*, 4
Unit-cell dimensions (Å)	$a = 7.2896(4)$, $b = 14.1435(5)$, $c = 10.1713(4)$
V (Å^3)	1048.68(7)
Absorption coefficient μ (mm^{-1})	11.834
F_{000}	1528
Data collection	
Crystal dimensions (mm)	0.03 × 0.10 × 0.33
Diffractometer	XCaliburS CCD
Radiation and wavelength (Å)	Mo*Kα*; 0.71073
θ range for data collection (°)	2.88–28.28
No. of measured, independent and observed [$I > 2\sigma(I)$] reflections	8442, 705, 691
h, *k*, *l* ranges	$-9 \le h \le 9$, $-18 \le k \le 18$, $-13 \le l \le 13$
R_{int}	0.0488
Absorption correction	Gaussian. Numerical absorption correction based on Gaussian integration over a multifaceted crystal model; Empirical absorption correction using spherical harmonics, implemented in *SCALE3 ABSPACK* scaling algorithm.
Refinement	
Data reduction	CrysAlisPro, Agilent Technologies, v. 1.171.37.34 (Agilent Technologies, 2014)
Structure solution	Direct methods
Refinement method	Full-matrix least-squares on F^2
Weighting coefficients *a*, *b*	0.0126, 15.0219
Extinction coefficient	0.00019(5)
Number of refined parameters	70
Final *R* indices [$I > 2\sigma(I)$]	$R_1 = 0.0303$, w$R_2 = 0.0633$
R indices (all data)	$R_1 = 0.0313$, w$R_2 = 0.0637$
GoF	1.279
$\Delta\rho_{max}$, $\Delta\rho_{min}$ (e^- Å^{-3})	1.19 and −1.01

$w = 1/[\sigma^2(Fo^2) + (aP)^2 + bP]$ where P is $[2Fc^2 + \mathrm{Max}(Fo^2, 0)]/3$.

Table 5. Coordinates, site multiplicities (*Q*), site populations, and equivalent and anisotropic thermal displacement parameters (U_{eq}, in Å^2), for stefanweissite.

Site	*Q*	*x*	*y*	*z*	Site population	U_{eq}	U^{11}	U^{22}	U^{33}	U^{23}	U^{13}	U^{12}
$^{VIII}M1$	8	¼	0.11714(4)	¾	$Ca_{0.544}Ce_{0.316}Th_{0.08}Mn_{0.06}$	0.00986(19)	0.0094(3)	0.0114(3)	0.0088(3)	0.000	0.0003(2)	0.000
$^{VII}M2$	8	½	0.23394(4)	0.01491(6)	$Zr_{0.96}Hf_{0.02}Mn_{0.02}$	0.0115(2)	0.0138(3)	0.0089(3)	0.0117(3)	−0.0020(2)	0.000	0.000
$^{VI}M3$	4	0	0.0	0	$Nb_{0.729(9)}Ti_{0.271(9)}$	0.0118(3)	0.0132(5)	0.0123(5)	0.0098(5)	0.0019(3)	0.000	0.000
$^{VI}M4$	8	¼	0.13370(6)	¼	$Ti_{0.78}Nb_{0.21}Al_{0.01}$	0.0133(2)	0.0182(5)	0.0098(4)	0.0120(4)	0.000	0.0046(4)	0.000
$^{IV}M5$	8	0.4181(11)	0.0	0	$Fe_{0.22}Mn_{0.03}$	0.0198(10)	0.015(4)	0.026(3)	0.018(4)	0.018(2)	0.000	0.000
$^{V}M6$	8	½	0.0130(6)	0.0359(10)	$Fe_{0.21}Mn_{0.04}$	0.045(2)	0.078(10)	0.021(4)	0.037(5)	0.021(3)	0.000	0.000
O1	16	0.1951(5)	0.0318(2)	0.1255(3)		0.0212(8)	0.033(2)	0.0148(15)	0.0160(16)	0.0008(13)	−0.0109(15)	−0.0074(15)
O2	16	0.2138(5)	0.2328(2)	0.1195(3)		0.0174(8)	0.028(2)	0.0119(15)	0.0124(16)	0.0026(12)	−0.0066(14)	0.0046(14)
O3	8	½	0.1073(3)	−0.0990(5)		0.0149(10)	0.017(2)	0.011(2)	0.017(2)	−0.0016(18)	0.000	0.000
O4	8	0	0.1287(3)	−0.0913(5)		0.0146(9)	0.012(2)	0.010(2)	0.021(2)	−0.0029(18)	0.000	0.000
O5	8	½	0.1368(4)	0.1764(5)		0.0220(11)	0.011(2)	0.033(3)	0.023(3)	0.014(2)	0.000	0.000

X-ray diffraction data of both samples correspond to the space group *Cmca*, and obviously they are isostructural. In the sample of nöggerathite-(Ce) Σ*REE* prevails over Ca at the *M*1 site, and on the basis of the Levinson rule this mineral should be considered as Ce-dominant (*REE* prevail over Ca in total and Ce prevails over other *REE*). In addition, in Sample 1 *REE* are the main charge-balancing component (and, consequently, can be considered as a species-defining component in the nöggerathite-(Ce) like Fe^{3+} in ferrihollandite, V^{3+} in mannardite, Sn^{4+} in nigerite-group minerals, K in barytolamprophyllite [for the site occupied as (Ba,Sr,K,Na)], Na in nabalamprophyllite [for the site occupied as (Ba,Na,Sr,K)] etc. On the other hand, in Sample 1 the sum of bivalent cations (Ca + Mn) prevails over

Table 6. Selected interatomic distances (Å) in the structure of stefanweissite.

*M*1–O3	2.388(3) ×2	*M*2–O4	2.092(4)	*M*3–O1	1.964(3) ×4
*M*1–O4	2.440(3) ×2	*M*2–O2	2.126(3) ×2	*M*3–O4	2.044(5) ×2
*M*1–O1	2.490(3) ×2	*M*2–O3	2.132(5)	<*M*3–O>	1.991
*M*1–O2	2.517(3) ×2	*M*2–O5	2.141(5)		
<*M*1–O>	2.458	*M*2–O2	2.342(4) ×2		
		<*M*2–O>	2.186		
*M*4–O2	1.948(3) ×2	*M*5–O3	1.917(5) ×2	*M*6–O3	1.818(9)
*M*4–O1	1.960(3) ×2	*M*5–O1	2.115(7) ×2	*M*6–O3	1.914(9)
*M*4–O5	1.971(2) ×2	<*M*5–O>	2.016	*M*6–O5	2.261(11)
<*M*4–O>	1.960			*M*6–O1	2.417(6) ×2
				<*M*6–O>	2.165

https://doi.org/10.1180/mgm.2018.171 Published online by Cambridge University Press

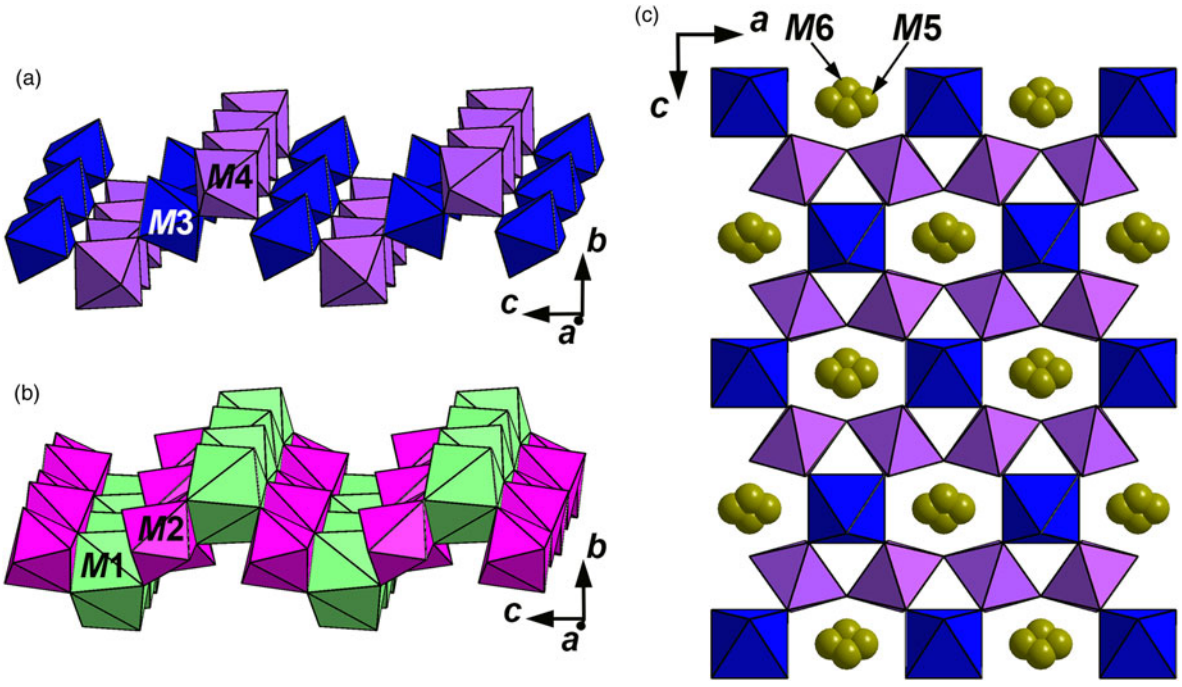

Fig. 3. Octahedral (*a*) and large-cation (*b*) layers and arrangement of Fe-dominant sites *M*5 and *M*6 inside the octahedral layer (*c*) in the structure of stefanweissite.

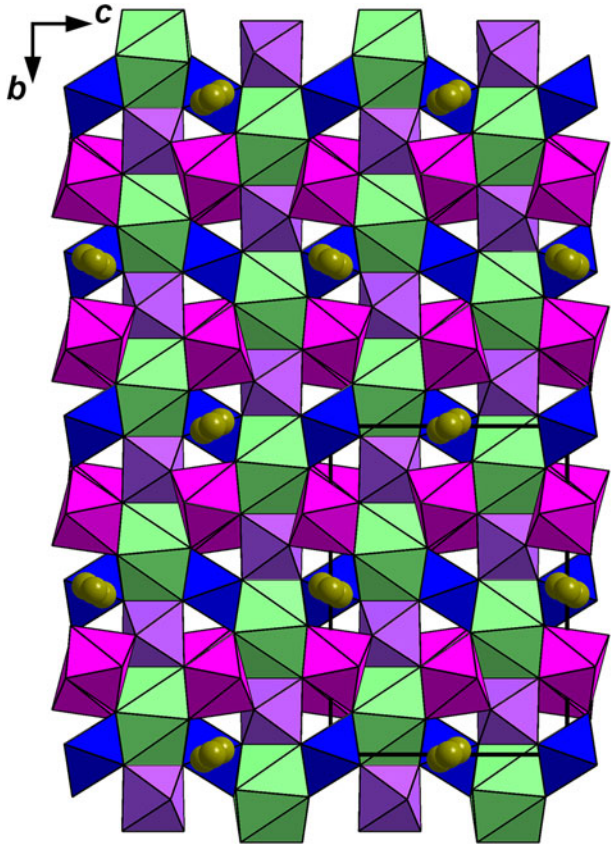

Fig. 4. The crystal structure of stefanweissite: general view. The unit cell is outlined. For legend see Fig. 3.

Σ*REE* at the *M*1 site. Consequently, in terms of the dominant-valency rule (Hatert and Burke, 2008) Sample 1 should be considered as a Ca-dominant mineral.

Sample 2 of nöggerathite-(Ce) is *REE*-dominant in terms of all nomenclature rules (i.e. dominant-valency rule, dominant-constituent rule, Levinson rule and charge-balancing component rule).

The dominant-valency rule was applied to some minerals with heterovalent substitutions at two sites, e.g. in the nomenclature systems for minerals of the amphibole, arrojadite and epidote groups (Hawthorne and Oberti 2006; Cámara *et al.* 2006; Chopin *et al.* 2006; Armbruster *et al.* 2006). However in minerals belonging to the nöggerathite-(Ce)–stefanweissite series coupled heterovalent–homovalent substitutions at four sites takes place: $(REE,Ca,Mn)_2(Zr,Mn)_2(Nb,Ti)(Ti,Nb)_2Fe^{2+}O_{14}$. As a result, the end-member formula $Ca_2Zr_2NbTi_2Fe^{2+}O_{14}$ written following the dominant-valency rule for a sample with *REE* > Ca but *REE* < Ca + Mn is not charge-balanced, and this is not the only case of a mineral that does not have an adequate end-member formula with one component at each site. This raises the question of how formulae of such minerals should be written. A way to solve this problem would be to write an end-member formula with two cations in the same site, as was done for the minerals of the lamprophyllite group: for example, the formula of lamprophyllite given in the IMA list of minerals (Pasero, 2018) updated in November 2018 is $(SrNa)Ti_2Na_3Ti(Si_2O_7)_2O_2(OH)_2$. This formula was accepted based on the fact that Na is the main charge-balancing univalent cation at the *A* site despite the fact that the Sr content prevails significantly over the Na content at this site. On the basis of this precedent, the end-member formulae of stefanweissite and nöggerathite-(Ce) could be written as $Ca_2Zr_2Nb(TiNb)Fe^{2+}O_{14}$ and $(CaCe)Zr_2NbTi_2Fe^{2+}O_{14}$, respectively.

The rules for writing end-member formulae in such complicated cases are not fully worked out, and appropriate guidelines made by the IMA CNMNC would be useful. This issue concerns not only zirconolite-related minerals. Such situations are numerous. For example, the end-member formula for alumoåkermanite $(Ca,Na)_2(Al,Mg,Fe^{2+})(Si_2O_7)$ with one cation at each site, i.e. $Ca_2Al(Si_2O_7)$, is not charge-balanced. The charge-balanced

https://doi.org/10.1180/mgm.2018.171 Published online by Cambridge University Press

Table 7. Comparative data for stefanweissite and related minerals.

Mineral	Stefanweissite	Nöggerathite-(Ce)	Zirconolite-3*O*	Laachite
Idealised formula	$(Ca,REE)_2Zr_2(Nb,Ti)(Ti,Nb)_2Fe^{2+}O_{14}$	$(Ce,Ca)_2Zr_2(Nb,Ti)(Ti,Nb)_2Fe^{2+}O_{14}$	$CaZrTi_2O_7$	$Ca_2Zr_2Nb_2TiFeO_{14}$
Crystal system	Orthorhombic	Orthorhombic	Orthorhombic	Monoclinic
Space group	*Cmca*	*Cmca*	*Cmca*	*C*2/*c*
a (Å)	7.2896	7.2985	7.278–7.284	7.3119
b (Å)	14.1435	14.1454	14.147–14.18	14.1790
c (Å)	10.1713	10.1607	10.145–10.148	10.1700
β (°)	90	90	90	90.072
Z	4	4	8	4
Strongest lines of the powder X-ray diffraction pattern: *d*, Å (*I*, %)	2.983 (100) 2.897 (71) 1.828 (38) 1.793 (25) 1.767 (16) 1.536 (9) 1.517 (10) 1.187 (19)	2.963 (91) 2.903 (100) 2.540 (39) 1.823 (15) 1.796 (51) 1.543 (20) 1.519 (16)	3.176 (30) 2.914 (100) 2.506 (40) 1.980 (90) 1.792 (90) 1.517 (10)	4.298 (22) 2.967 (100) 2.901 (59) 2.551 (32) 1.800 (34) 1.541 (24) 1.535 (23) 1.529 (23)
Refractive index	2.260 (mean, calc.)	2.267 (mean, calc.)	2.215 (meas., metamict) 2.26–2.31 (calc.)	2.26 (mean, calc.)
Density (g cm^{-3})	5.254 (calc.)	5.332 (calc.)	4.7 (meas., metamict) 4.9 (calc.)	5.42 (calc.)
Sources	[1]	[2]	[3]	[4]

Sources: [1] This work. [2] Chukanov *et al.* (2018*a*). [3] Borodin *et al.* (1956); Chukhrov and Bonshtedt-Kupletskaya (1967); Pudovkina *et al.* (1969); Sinclair and Eggleton (1982); Mazzi and Munno (1983); Bayliss *et al.* (1989); Della Ventura *et al.* (2000). [4] Chukanov *et al.* (2014).

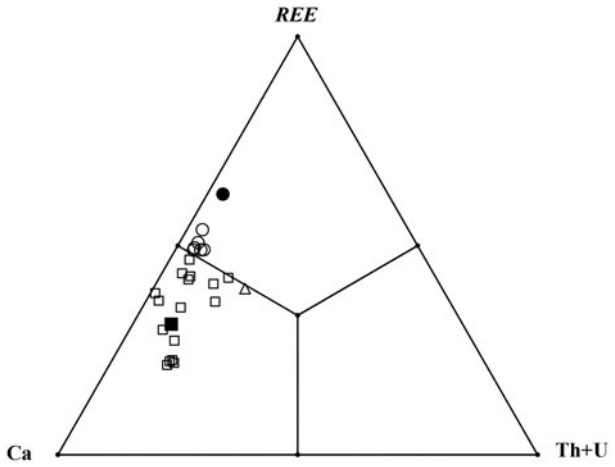

Fig. 5. Ratios of large $^{VIII}M1$ cations in orthorhombic zirconolite-type minerals from the Laach Lake volcano: the holotype stefanweissite (black square); other stefanweissite samples (open squares); and nöggerathite-(Ce) (open circles – our data; black circle – analysis 1 from Della Ventura *et al.*, 2000).

formula would be $(CaNa)Al(Si_2O_7)$. The other well-known examples are loparite-(Ce) and melanostibite with the idealised formulae $(NaREE)Ti_2O_6$ and $Mn^{2+}(Sb^{5+},Fe)O_3$ [$= Mn^{2+}(Sb^{5+}_{0.5}Fe^{3+}_{0.5})O_3$ i.e., with Sb and Fe in the same site], respectively. This is only a small number of examples to illustrate this nomenclature problem.

It is important to note that nöggerathite-(Ce) (the richest in *REE*), was actually described by Della Ventura *et al.* (2000) before the approval of this mineral. It is orthorhombic [with $a = 7.284(5)$, $b = 14.18(8)$ and $c = 10.145(8)$ Å], with the empirical formula (ranges): $Ca_{0.312–0.337}Y_{0.079–0.093}La_{0.069–0.086}Ce_{0.269–0.296}Pr_{0.020–0.028}Nd_{0.052–0.062}Sm_{0.004–0.006}Gd_{0.005–0.006}Dy_{0.003–0.006}Er_{0.003–0.005}Th_{0.014–0.073}U_{0.008–0.022}Mn_{0.345–0.397}Mg_{0.003–0.005}Al_{0.020–0.025}Fe_{0.301–0.339}Zr_{0.888–0.910}Hf_{0.006–0.009}Ti_{0.840–0.888}Nb_{0.575–0.613}Ta_{0.007–0.009}Si_{0.000–0.012}O_{7.000}$. In particular, the empirical formula corresponding to spot analysis number 1 from the paper by Della Ventura *et al.* (2000), calculated on 14 O apfu is $(REE_{1.14}Ca_{0.63}Mn_{0.17}Th_{0.04}U_{0.02})_{\Sigma 2}[(Fe_{0.65}Mn_{0.55}Al_{0.05}Mg_{0.01})_{\Sigma 1.26}(Zr_{1.79}Hf_{0.01})_{\Sigma 1.8}(Ti_{1.71}Nb_{1.19}Ta_{0.02})_{\Sigma 2.92}Si_{0.02}]_{\Sigma 6}O_{14}$. These data confirm that the existence of nöggerathite-(Ce) as a *REE*-dominant mineral and its distinction from stefanweissite are undeniable.

Comparative data for stefanweissite, nöggerathite-(Ce), zirconolite-3*O* and laachite are given in Table 7. A spread of compositions between stefanweissite and nöggerathite-(Ce) is shown in Fig. 5.

Among the analyses of ~300 zirconolite samples compiled by Williams and Gieré (1996), there are only a minor number where the content of Nb_2O_5 exceeds 10 wt.%. Unlike zirconolite, stefanweissite, laachite and nöggerathite-(Ce) contain niobium as a species-defining component. The composition of a mineral with Nb:Ti ≈ 43:57 from Vuoriyarvi, Northern Karelia, Russia described by Borodin *et al.* (1960) as 'niobozirconolite' corresponds to stefanweissite.

Acknowledgements. This work was supported by the Russian Science Foundation, grant no. 14-17-00048 (in part for the chemical study of stefanweissite and other zirconolite-type minerals) and Russian Foundation for Basic Research, grant no. 18-29-12007 (in parts for mineralogical study, Raman spectroscopy and X-ray structural analysis). The authors thank the X-ray Diffraction Centre of Saint-Petersburg State University for instrumental and computational resources.

Supplementary material. To view supplementary material for this article, please visit https://doi.org/10.1180/mgm.2018.171.

References

Agilent Technologies (2014) *CrysAlisPro, v. 1.171.37.34.* Agilent Technologies, Yarnton, Oxfordshire, UK.

Armbruster T., Bonazzi P., Akasaka M., Bermanec V., Chopin C., Gieré R., Heuss- Assbichler S., Liebscher A., Menchetti S., Pan Yuanming and Pasero M. (2006) Recommended nomenclature of epidote-group minerals. *European Journal of Mineralogy*, **18**, 551–567.

Barinova T.V., Borovinskaya I.P., Ratnikov V.I. and Ignat'eva T.I. (2008) Self-propagating high-temperature synthesis for immobilization of high-level waste in mineral-like ceramics: 1. Synthesis and study of titanate ceramics based on perovskite and zirconolite. *Radiochemistry*, **50**, 316–320.

Bayliss P., Mazzi F., Munno R. and White T.J. (1989) Mineral nomenclature: zirconolite. *Mineralogical Magazine*, **53**, 565–569.

Berzelius J. (1824) Undersökning af några Mineralier. 2. Polymignit. *Kongliga Svenska Vetenskaps-Academiens Handlingar*, 338–345.

Borodin L.S., Bykova A.V., Kapitonova T.A. and Pyatenko Y.A. (1960) New data on zirconolite and its new niobian variety. *Doklady Akademii Nauk SSSR*, **134**, 1188–1192.

Brøgger W.C. (1890) Die Mineralien der Syenitpegmatitgänge der südnorwegischen Augit und Nephelinsyenite. *Zeitschrift für Kristallographie, Speziellen Teil*, **16**, 1–663.

Cámara F., Oberti R., Chopin C. and Medenbach O. (2006) The arrojadite enigma. I. A new formula and a new model for the arrojadite structure. *American Mineralogist*, **91**, 1249–1259.

Chopin C., Oberti R. and Cámara F. (2006) The arrojadite enigma. II. Compositional space, new members, and nomenclature of the group. *American Mineralogist*, **91**, 1260–1270.

Chukanov N.V., Krivovichev S.V., Pakhomova A.S., Pekov I.V., Schäfer Ch., Vigasina M.F. and Van K.V. (2014) Laachite, $(Ca,Mn)_2Zr_2Nb_2TiFeO_{14}$, a new zirconolite-related mineral from the Eifel volcanic region, Germany. *European Journal of Mineralogy*, **26**, 103–111.

Chukanov N.V., Zubkova N.V., Britvin S.N., Pekov I.V., Vigasina M.F., Schäfer C., Ternes B., Schüller W., Ermolaeva V.N. and Pushcharovsky D.Y. (2018*a*) Nöggerathite-(Ce), $(Ce,Ca)_2Zr_2(Nb,Ti)(Ti,Nb)_2Fe^{2+}O_{14}$, a new zirconolite-related mineral from the Eifel volcanic region, Germany. *Minerals*, **8**(10), 449; https://doi.org/10.3390/min8100449.

Chukanov N.V., Zubkova N.V., Britvin S.N., Pekov I.V., Vigasina M.F., Schäfer C., Ternes B., Schüller W., Ermolaeva V.N. and Pushcharovsky D.Y. (2018*b*) Nöggerathite-(Ce), IMA 2017-107. CNMNC Newsletter No. 42, April 2018, page 448; *Mineralogical Magazine*, **82**, 445–451.

Chukanov N.V., Zubkova N.V., Pekov I.V., Vigasina M.F., Polekhovsky Y.S., Ternes B., Schüller W., Britvin S.N. and Pushcharovsky D.Y. (2018*c*) Stefanweissite, IMA 2018-020. CNMNC Newsletter No. 44, August 2018, page 1016; *Mineralogical Magazine*, **82**, 1015–1021.

Chukhrov F.V. and Bonshtedt-Kupletskaya E.M. (1967) *Minerals*. Nauka, Moscow, volume II(3) [in Russian].

Della Ventura G., Bellatreccia F. and Williams C.T. (2000) Zirconolite with significant *REE*ZrNb(Mn,Fe)O_7 from a xenolith of the Laacher See eruptive center, Eifel volcanic region, Germany. *The Canadian Mineralogist*, **38**, 57–65.

Donald I.W., Metcalfe B.L. and Taylor R.N.J. (1997) The immobilization of high level radioactive wastes using ceramics and glasses. *Journal of Materials Science*, **32**, 5851–5887.

Geisler T., Zhang M. and Salje E.K. (2003) Recrystallization of almost fully amorphous zircon under hydrothermal conditions: an infrared spectroscopic study. *Journal of Nuclear Materials*, **320**, 280–291.

Hatert F. and Burke E.A.J. (2008) The IMA-CNMNC dominant-constituent rule revisited and extended. *The Canadian Mineralogist*, **46**, 717–728.

Hawthorne F.C. and Oberti R. (2006) On the classification of amphiboles. *The Canadian Mineralogist*, **44**, 1–21.

Hurai V., Huraiová M., Gajdošová M., Konečný P., Slobodník M. and Siegfried P.R. (2018) Compositional variations of zirconolite from the Evate apatite deposit (Mozambique) as an indicator of magmatic-hydrothermal conditions during post-orogenic collapse of Gondwana. *Mineralogy and Petrology*, **112**, 279–296.

Laverov N.P., Yudintsev S.V., Stefanovsky S.V., Omel'yanenko B.I. and Nikonov B.S. (2006) Murataite as a universal matrix for immobilization of actinides. *Geology of Ore Deposits*, **48**, 335–356.

Litt T., Brauer A., Goslar T., Merk J., Balaga K., Mueller H., Ralska-Jasiewiczowa M., Stebich M. and Negendank J.F.W. (2001) Correlation and synchronisation of Lateglacial continental sequences in northern Central Europe based on annually laminated lacustrine sediments. Pp. 1233–1249 in: *Integration of Ice Core, Marine and Terrestrial Records of Termination 1 from the North Atlantic Region.* (S. Bjorck, J.J. Lowe and M.J.C. Walker, editors). Quaternary Science Reviews, Vol. 20.

Lumpkin G.R., Gao Y., Giere R., Williams C.T., Mariano A.N. and Geisler T. (2014) The role of Th-U minerals in assessing the performance of nuclear waste forms. *Mineralogical Magazine*, **78**, 1071–1095.

Mazzi F. and Munno R. (1983) Calciobetafite (new mineral of the pyrochlore group) and related minerals from Campi Flegrei, Italy; crystal structures of polymignite and zirkelite: comparison with pyrochlore and zirconolite. *American Mineralogist*, **68**, 262–276.

Pasero M. (2018) *The New IMA List of Minerals*. http://nrmima.nrm.se/

Pudovkina Z.V., Chernitzova N.M. and Pyatenko Y.A. (1969) Crystallographic study of polymignyte. *Zapiski Vsesoiuznogo Mineralogicheskogo Obshchestva*, **98**, 193–199 [in Russian].

Ringwood A.E. and Kelly P.M. (1986) Immobilization of high-level waste in ceramic waste forms. *Philosophical Transactions of the Royal Society of London A*, **319**, DOI: 10.1098/rsta.1986.0086.

Salamat A., McMillan P.F., Firth S., Woodhead K., Hector A.L., Garbarino G., Stennett M.C. and Hyatt N.C. (2013) Structural transformations and disordering in zirconolite ($CaZrTi_2O_7$) at high pressure. *Inorganic Chemistry*, **52**, 1550–1558.

Schmitt A.K., Wetzel F., Cooper K.M., Zou H. and Wörner G. (2010) Magmatic longevity of Laacher See volcano (Eifel, Germany) indicated by U–Th dating of intrusive carbonatites. *Journal of Petrology*, **51**, 1053–1085.

Williams C.T. and Gieré R. (1996) Zirconolite: a review of localities worldwide, and a compilation of its chemical compositions. *Bulletin of the Natural History Museum London* (*Geology*), **52**, 1–24.

Zhang Y., Gregg D.J., Kong L., Jovanovich M. and Triani G. (2017) Zirconolite glass-ceramics for plutonium immobilization: The effects of processing redox conditions on charge compensation and durability. *Journal of Nuclear Materials*, **490**, 238–241.

Zubkova N.V., Chukanov N.V., Pekov I.V., Ternes B., Schüller W. and Pushcharovsky D.Yu. (2018) The crystal structure of nonmetamict Nb-rich zirconolite-3*T* from the Eifel paleovolcanic region, Germany. *Zeitschrift für Kristallografie*, **233**, 463–468.

https://doi.org/10.1180/mgm.2018.171 Published online by Cambridge University Press